The effect of high pressure on the FM properties of I is essentially explained by the pressure dependence of the intermolecular overlap integrals between SOMO–NHOMO and/or between SOMO–NLUMO. This fact further confirms that the FM intermolecular interaction results from the intermolecular orbital overlaps, i.e., CT interaction.

Summary

The effect of hydrostatic high-pressure on the temperature dependence of the static magnetic susceptibility and the field dependence of the magnetization of the FM organic radical I indicates a pressure-induced enhancement of the FM intermolecular interaction. The FM coupling is increased by 40% at a pressure of 9 kbar. This rather large change suggests the possibility that the high-pressure prompts a phase transition into a 3-D FM ordered state in the FM organic solid. The pressure dependence of the FM interaction in I is approximately interpreted in terms of an increase in the intermolecular overlap integrals between SOMO/NHOMO and/or between SOMO/NLUMO by the application of pressure.

This work indicates that high-pressure experiments are useful and interesting in the study of organic/molecular ferromagnetism. Studies of the high-pressure effects on other FM systems are now in progress.

Acknowledgment. We thank Dr. K. Imaeda of the Institute for Molecular Science (IMS) for his helpful discussions and the pressure calibration of the Be–Cu clamp cell. We thank Mr. S. Bandow of IMS for his kind help in the setup of the Faraday susceptometer system. We are grateful to Dr. T. Inabe and Mr. T. Ida of IMS for their helpful discussions.

Registry No. I, 38582-73-9.

Influence of Cryptands and Crown Ethers on Ion Transport and Vibrational Spectra of Polymer–Salt Complexes

Kate E. Doan, Bruce J. Heyen, M. A. Ratner,* and D. F. Shriver*

Department of Chemistry and Materials Research Center, Northwestern University, Evanston, Illinois 60208-3113

Received March 27, 1990

Complex impedance data demonstrate that addition of 2.2.2-cryptand increases the conductivity of $NaSO_3CH_3$ in amorphous poly(ethylene oxide) (aPEO) but decreases that of $NaSO_3CF_3$ in aPEO. Vibrational spectroscopic and X-ray diffraction measurements indicate that the influence of 2.2.2-cryptand is to dissolve crystallites of $NaSO_3CH_3$ into the polymer phase. The decrease in conductivity for $NaSO_3CF_3$–aPEO upon addition of 2.2.2-cryptand correlates with the precipitation of a crystalline phase, presumably [Na:2.2.2][SO_3CF_3].

Introduction

Solvent-free polymer electrolytes exhibiting high ionic conductivities are amorphous materials and are therefore difficult to characterize structurally.[1,2] Information about the mechanism of ion conduction in solvent-free polymer electrolytes has been obtained by physical measurements on chemically modified series of electrolytes. Chemical modifications include the synthesis of amorphous host polymers with low glass transition temperatures, T_g's,[3,4] the addition of plasticizers to reduce the T_g of polymer–salt complexes,[5,6] and the preparation of amorphous forms of PEO.[7-9]

Polymer electrolytes can be regarded as concentrated salt solutions in a medium with local solvent mobility but negligible long-range solvent motion. The dielectric constant of the host polymer is low and is implicated as a factor that reduces conductivity.[10] Spectroscopic studies indicate that there is considerable cation–anion interaction in polymer–salt complexes.[11-13] One chemical modification aimed specifically at reducing ion pairing is the addition of cation complexing agents, such as crown ethers or cryptands to polymer–salt complexes[14] or polyelectrolytes.[15,16] These complexing agents have been observed to enhance the conductivity 10–1000-fold. The nature of the conductivity enhancement has not been well elucidated. It is commonly supposed that the main influence of the complexing agent is to decrease ion pairing by in-

(1) Armand, M. B. *Annu. Rev. Mater. Sci.* **1986**, *16*, 245.
(2) *Polymer Electrolyte Reviews*; MacCallum, J. R., Vincent, C. A., Eds.; Elsevier Applied Science: New York, 1987; Vol. 1.
(3) Blonsky, P. M.; Shriver, D. F.; Austin, P. E.; Allcock, H. R. *J. Am. Chem. Soc.* **1984**, *106*, 6854.
(4) Spindler, R.; Shriver, D. F. *Macromolecules* **1988**, *21*, 648.
(5) Spindler, R.; Shriver, D. F. *Macromolecules* **1986**, *19*, 347.
(6) Tsuchida, E.; Ohno, H.; Tsunemi, K.; Kobayashi, N. *Solid State Ionics* **1983**, *11*, 227.
(7) Nicholas, C. V.; Wilson, D. J.; Booth, C.; Giles, J. R. M. *Brit. Polym. J.* **1988**, *20*, 289.
(8) Watanabe, M.; Itoh, M; Sanui, K.; Ogata, N. *Macromolecules* **1987**, *20*, 569.
(9) Giles, J. R. M.; Greenhall, M. P. *Polym. Commun.* **1986**, *27*, 360.
(10) MacCallum, J. R.; Tomlin, A. S.; Vincent, C. A. *Eur. Polym. J.* **1986**, *22*, 787.
(11) (a) Papke, B. L.; Dupon, R.; Ratner, M. A.; Shriver, D. F. *Solid State Ionics* **1981**, *5*, 685. (b) Dupon, R.; Papke, B. L.; Ratner, M. A.; Whitmore, D. H.; Shriver, D. F. *J. Am. Chem. Soc.* **1982**, *104*, 6247.
(12) Teeters, D.; Frech, R. *Solid State Ionics* **1986**, *18–19*, 271.
(13) (a) Borjesson, L.; Martin, S. W.; Torell, L. M.; Angell, C. A. *Solid State Ionics* **1986**, *18–19*, 431. (b) Schantz, S.; Sandahl, J.; Borjesson, L.; Torell, L. M.; Stevens, J. R. *Solid State Ionics* **1988**, *28–30*, 1047. (c) Schantz, S.; Torell, L. M.; Stevens, J. R. *J. Appl. Phys.* **1988**, *64*, 2038.
(14) Kaplan, M. L.; Rietman, E. R.; Cava, R. J.; Holt, L. K.; Chandross, E. A. *Solid State Ionics* **1987**, *25*, 37.
(15) Chen, K.; Ganapathiappan, S.; Shriver, D. F. *Chem. Mater.* **1989**, *1*, 483.
(16) Zhou, G.; Khan, I. M.; Smid, J. *Polym. Prepr., Div. Polym. Chem. Am. Chem. Soc.* **1989**, *30*(1), 416.

0897-4756/90/2802-0539$02.50/0 © 1990 American Chemical Society

creasing the distance of the closest approach of the cation and anion.

This paper describes parallel conductivity and spectroscopic studies designed to explore the role of complexing agents on ion pairing and conductivity. For reasons outlined below this study focuses on polymer–salt complexes of $NaCH_3S_3$ and $NaCF_3SO_3$ with oxymethylene-linked poly(ethylene oxide),[7] here referred to as aPEO (for amorphous poly(ethylene oxide)). Additionally, the effects of cryptand addition to aPEO complexes of NaI, NaSCN, and $NaBF_4$ have been investigated.

The salts $NaCH_3SO_3$ and $NaCF_3SO_3$ were chosen because of their similer anion size but different basicities. For example, the conjugate acid of $CF_3SO_3^-$, HCF_3SO_3 will protonate H_2SO_4,[17] whereas HCH_3SO_3 is a slightly weaker acid than H_2SO_4.[18] This difference in basicity should be reflected on the tendencies of the salts to ion pair. Additionally, the extent of cation interaction with these anions can be probed by monitoring the symmetric stretch of the SO_3 moiety. Torell has demonstrated that in $PPO_xNaCF_3SO_3$ electrolytes this band splits as the salt concentration is increased.[13b] In addition, three reports have appeared on conductivity enhancement by the addition of cation complexing agents to polymer electrolytes containing RSO_3^- anions.[14-16]

The salts NaSCN, NaI, and $NaBF_4$ were chosen for comparative study because spectroscopic studies indicate that there is ion pairing in PEO complexes with NaSCN, whereas in $NaBF_4$ complexes there is no evidence for strong ion–ion interaction.[14,15] Although the NaI complexes are difficult to characterize by vibrational spectroscopy, oriented fiber diffraction studies on high-concentration semicrystalline PEO complexes indicate there are close Na^+–I^- interactions.[19]

The polymer aPEO (I) is structurally the simplest of the polymer host materials that forms complexes with high room-temperature conductivity. Although the host

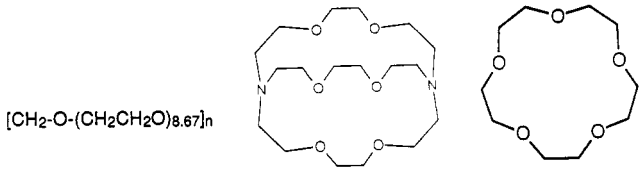

polymer was reported in 1986,[20] a convenient synthesis has been reported only recently.[7] The cation complexing agents used in this study 2.2.2-cryptand ([2.2.2], II), and 15-crown-5 (15C5, III), are macrocyclic ligands known to form very strong complexes with alkali-metal cations; they have been widely used to solvate alkali-metal salts in low-polarity media.[21,22] Although [2.2.2] shows highest specificity for binding K^+, it also forms strong complexes with Na^+.[22]

Experimental Section

Materials. The polymer aPEO was prepared from the reaction of poly(ethylene glycol), PEG(400), with excess KOH in CH_2Cl_2 by using procedures described by Nicholas.[7] Molecular weight determinations were performed at General Motors Research Laboratory by size exclusion chromatography column on THF solutions (M_n = 6500, M_w = 22700). Molecular weights were referenced to THF solutions of polystyrene. The salts $NaCF_3SO_3$, NaSCN, NaI, and $NaBF_4$ (Alpha or Aldrich) were recrystallized from methanol and dried at 50 °C under vacuum for 2 days. Sodium methanesulfonate was prepared by neutralizing aqueous HCH_3SO_3 with sodium hydroxide and then recrystallized from methanol and dried at 50 °C under vacuum. Reagent grade methanol (MCB) was dried by reflux over iodine-activated magnesium and distilled under a dry-nitrogen atmosphere. The 15-crown-5 and cryptand ([2.2.2], Aldrich) were used as received.

Complex Formation. Salt complexes were prepared by the addition of methanol to stoichiometric quantities of salt, polymer, and crown ether or cryptand in a reaction vessel under an inert atmosphere. The mixture was stirred until a homogeneous solution was obtained. Upon removal of the solvent the salt complexes were dried under vacuum at 60 °C for 2 days and then stored in a dry inert atmosphere.

Physical Characterization of Complexes. Differential scanning calorimetry (DSC) was performed on a Perkin-Elmer DSC 2 equiped with liquid N_2 cooling. Samples were loaded into hermetically sealed aluminum pans. The instrument was calibrated by using four standards (gallium, cyclohexane, decane, and heptane). Transitions were measured at three heating rates, normally 80, 40, and 20 °C/min. Glass transitions were taken as the midpoint of the inflection; melts and cold crystallization were taken as the peak of the transition. All transitions including melting crystallization and glass transitions were extrapolated to heating rate of 0 °C/min to yield the reported values for the transitions.[5] X-ray powder diffraction traces were obtained at room temperature on a Rigaku automated powder diffractometer using Cu Kα radiation.

Raman spectra were recorded by using a filtered argon-ion 514.5-nm line for illumination and a Spex 1401 monochromator with photon-counting detection.[23] All samples were probed with 180° backscattering geometry. Raman shifts were measured relative to the exciting line. The spectral resolution was normally 3 cm^{-1}. To reduce the background fluorescence the spectra were run without spinning and the samples were usually laser bleached for 10 min before the spectra were recorded.

Infrared spectra were recorded on an Alpha-Centauri Mattson FT-IR with a DTGS detector. Thin film samples were cast from methanol onto CaF_2 or ZnS plates. The films were then dried under vacuum for 1 day before the spectra were recorded. Spectral resolution was normally 4 cm^{-1}.

Samples for ac impedance analysis were pressed into pellets inside spring-loaded air-tight conductivity cells between stainless-steel electrodes. The frequency-dependent impedance was measured on an HP 4192 impedance analyzer (5 Hz–5 MHz). The sample cells were placed in a regulated air bath (±0.1 °C) for the temperature control. To ensure good contact between the electrodes and the sample, the loaded cells were heated at 80 °C overnight, before dielectric measurements were made.

Temperature-dependent conductivities were fit by the VTF equation, eq 4, and the Arrhenius equation, eq 5, by using linear least-squares methods. To fit the data by the VTF equation, the parameter T_0 was changed iteratively until a best fit could be obtained, as judged by the correlation coefficient, r.

Results and Discussion

Formation and Characterization of Polymer–Salt Complexes. Polymer–salt complexes of stoichiometries 25, 12, and 8 ethylene oxide units/salt formula unit were studied in the $NaCF_3SO_3$ system. Compositions of 25 and 8 ethylene oxide units/salt formula unit were studied in the $NaCH_3SO_3$ system. Only low-concentration complexes (25 EO units/salt formula unit) were studied for the other salts. X-ray diffraction patterns indicate that aPEO and its complexes with $NaCF_3SO_3$, $NaBF_4$, NaI, and NaSCN are amorphous. The $NaCH_3SO_3$ complexes, even at low salt concentration ($aPEO_{25}NaCH_3SO_3$), contain excess salt

(17) Howells, D.; McCown, J. D. *Chem. Rev.* **1977**, *77*, 69.
(18) Kice, J. L. *Adv. Phys. Org. Chem.* **1980**, *72*, 132.
(19) Okamura, S.; Chatani, Y. *Polymer* **1987**, *28*, 1815.
(20) Craven, J. R.; Mobbs, R. H.; Booth, C.; Giles, J. R. M. *Makromol. Chem. Rapid Commun.* **1986**, *7*, 81.
(21) Lehn, J. *Acc. Chem. Res.* **1978**, *11*(2), 1.
(22) Izatt, R. M.; Eatough, D. J.; Christensen, J. J. *Struct. Bonding* **1973**, *16*, 161.
(23) Hardy, L. C.; Shriver, D. F. *J. Am. Chem. Soc.* **1986**, *108*, 2887.

Table I. Thermal Transitions of aPEO and Its Complexes

polymer	$T_g \pm 2$, K	$T_{cc} \pm 3$, K	$T_{m1} \pm 3$, K	$T_{m2} \pm 3$, K
aPEO	211	219	286	294
$aPEO_{25}NaCF_3SO_3$	224			
$aPEO_{12}NaCF_3SO_3$	236			
$aPEO_8NaCF_3SO_3$	244			
$aPEO_{25}NaCH_3SO_3$	212	br[a]	281	br
$aPEO_{25}NaBF_4$	223			
$aPEO_{25}NaI$	229			
$aPEO_{25}NaSCN$	227			
$aPEO_{25}(NaCF_3SO_3$:[2.2.2])	214	221	283	br
$aPEO_{25}(NaCF_3SO_3$:0.5[2.2.2])	213		273	
$aPEO_{25}(NaCF_3SO_3$:(15C5))	210	227	br	291
$aPEO_{25}(NaCH_3SO_3$:[2.2.2])	213		284	
$aPEO_{25}(NaCH_3SO_3$:0.5[2.2.2])	211		281	
$aPEO_{25}(NaCH_3SO_3$:(15C5))	206	221	br	288
$aPEO_{25}(NaBF_4$:[2.2.2])	208	224	br	288
$aPEO_{25}(NaI$:[2.2.2])	208	221	br	290
$aPEO_{25}(NaSCN$:[2.2.2])	208	221	279	290

[a] Broad.

as detected by X-ray diffraction. This indicates that $NaCF_3SO_3$ is strongly complexed by the polymer and is soluble to quite high concentrations, but $NaCH_3SO_3$ is virtually insoluble in the polymer.

The thermal behavior of the complexes also shows the different tendency of the polymer to solvate these salts (Table I). The polymer aPEO has a complicated DSC trace with a glass transition, a cold crystallization exotherm, and two melting endotherms occurring below room temperature. The complexes with $NaCF_3SO_3$, NaI, NaSCN, and $NaBF_4$ display only a glass transition. Apparently complex formation with these salts decreases the tendency of the polymer to form an ordered crystalline phase. It is interesting to note that the complexes of the strongly complexed salts with smaller anions have the highest T_g's. Watanabe has seen similar trends in complexes of PEO networks and lithium salts.[8] The $NaCH_3SO_3$ complex shows no significant rise in T_g when compared to aPEO, and although the other transitions due to the crystalline phase are broadened in the DSC trace they are still present.

Vibrational Spectroscopic Investigation of Anion–Cation Interaction. Spectroscopic studies of anion vibrational modes are commonly used to probe ion pairing in nonaqueous solutions. Generally, nondegenerate vibrational bands split at high salt concentrations; the new band usually appears at frequencies closer to the solid salt than the band due to the free ion.[24] This is indeed seen in the complexes of aPEO with $NaCF_3SO_3$. Figure 1 shows the Raman spectra of $NaCF_3SO_3$ and the salt complex with aPEO. In the complex $aPEO_8NaCF_3SO_3$ (Figure 1A), the vibrational bands due to ν(CS)(318, 331 cm^{-1}) $\delta_s(CF_3)$ (759, 770 cm^{-1}), and $\nu_s(SO_3)$ (1043, 1056 cm^{-1}) are split into two components;[25] the higher energy bands occur 10–15 cm^{-1} closer to those observed for solid $NaCF_3SO_3$ (ν(CS) 335 cm^{-1}, $\delta_s(CF_3)$ 79 cm^{-1}, $\nu_s(SO_3)$ 1067 cm^{-1}) than the lower energy bands. (The broad bands in the spectrum of the polymer–salt complex are due to vibrations of the host polymer aPEO). In the low salt concentration complex $aPEO_{25}NaCF_3SO_3$ only the low-frequency component of the three split bands is observed (ν_s(CS) 316 cm^{-1}, $\delta_s(CF_3)$ 759 cm^{-1}, $\nu_s(SO_3)$ 1043 cm^{-1}). Torell has seen similar behavior in $PPO_xNaCF_3SO_3$ complexes.[13b] These results suggest that in the high salt concentration complex, $aPEO_8NaCF_3SO_3$, there is considerable cation–anion interaction, but little if any contact ion pairing is present

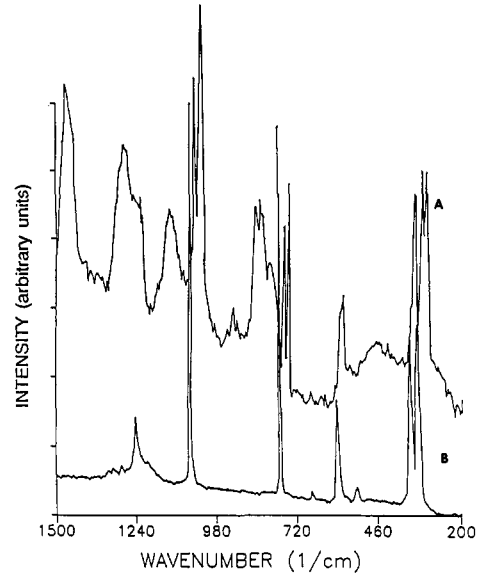

Figure 1. Raman spectra of aPEO–$NaCF_3SO_3$ complexes: (A) $aPEO_8NaCF_3SO_3$, (B) $NaCF_3SO_3$ (s).

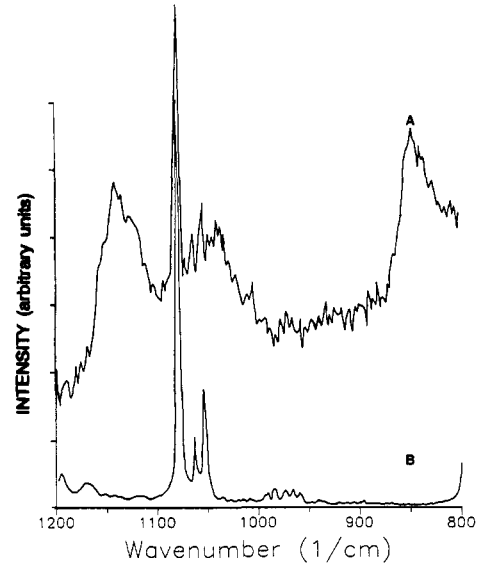

Figure 2. Raman spectra of (A) $aPEO_{25}NaCH_3SO_3$, (B) $NaCH_3SO_3$ (s).

(24) Irish, D. E. In *Ionic Interactions*; Petrucci, S., Ed.; Academic Press: New York, 1971; Vol. II.
(25) Miles, M. G.; Doyle, G.; Cooney, R. P.; Tobias, R. S. *Spectrochim. Acta* **1969**, *25A*, 1515.

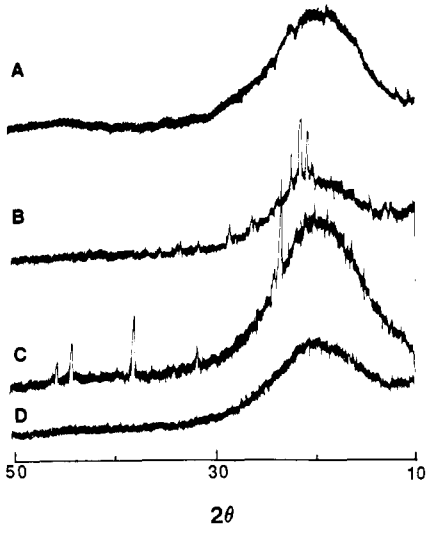

Figure 3. X-ray diffraction patterns for aPEO complexes: (A) $aPEO_{25}NaCF_3SO_3$, (B) $aPEO_{25}(NaCF_3SO_3$:[2.2.2]), (C) $aPEO_{25}NaCH_3SO_3$, (D) $aPEO_{25}(NaCH_3SO_3$:[2.2.2]).

in the low-concentration complex, $aPEO_{25}NaCF_3SO_3$. In the $NaCH_3SO_3$ complex the strongest band corresponds to that observed for the crystalline solid (Figure 2). (Due to interference by the background fluorescence in the spectra of the $NaCH_3SO_3$ complexes only the SO_3 symmetric stretching modes are reported.) The unchanged position of the SO_3 symmetric stretch at 1085 cm^{-1} indicates that the environment around the $CH_3SO_3^-$ anion resembles that in the crystalline solid, indicating considerable cation–anion interaction.

Satisfactory Raman spectra of the NaSCN and $NaBF_4$ complexes could not be obtained because of the fluorescence of these samples. Infrared spectroscopy was used instead to probe the anion environment. The CN stretch of the SCN^- ion occurs at 2059 cm^{-1} in the complex $aPEO_{25}NaSCN$ corresponding to that reported for a free anion in nonaqueous solutions.[26] The band due to ion pairs is commonly found at 2075 cm^{-1}. Contact ion pairing may still occur in this electrolyte because the band is rather broad (fwhm = 35 cm^{-1}) and thus may obscure a feature due to the presence of some ion-pairs. The strongest IR band for the BF_4^- ion, the asymmetric stretch, overlaps with bands due to the polymer and thus cannot be assigned.

Formation and Characterization of Cryptand Complexes. The addition of cryptand [2.2.2] to the polymer–salt complexes alters the solubility of the salts in aPEO, with the change in solubility being strongly dependent upon the salt. The addition of cryptand to complexes with $NaCF_3SO_3$, $NaBF_4$, NaI and NaSCN actually reduces the solubility of these salts in the polymer. This is shown by the appearance of peaks in the X-ray diffraction pattern of the electrolytes containing cryptand. By contrast, cryptand addition increases the solubility of $NaCH_3SO_3$ in the polymer and the complex $aPEO_{25}(NaCH_3SO_3$:[2.2.2]) is totally amorphous. The diffraction patterns for $NaCF_3SO_3$ and $NaCH_3SO_3$ complexes of aPEO with and without [2.2.2] are illustrated in Figure 3. The X-ray diffraction peaks observed in the complex $aPEO_{25}(NaCF_3SO_3$:[2.2.2]) match those of a pure $NaCF_3SO_3$:[2.2.2] complex. (*d* spacings for the most prominent diffraction peaks for $aPEO_{25}(NaCF_3SO_3$:[2.2.2]): 4.29 s, 4.15 s, 3.99 m, 3.40 m, 3.13 w, 2.85 w, 2.67 w Å.) Similarly, the $aPEO_{25}NaCH_3SO_3$ diffraction peaks correspond to pure $NaCH_3SO_3$. (Prominent *d* spacings for $aPEO_{25}NaCH_3SO_3$ are 4.60 m, 4.29 m, 3.69 s, 2.34 m, 2.05 m Å.) These results unambiguously confirm the identity of the undissolved species in the polymer–salt complexes. Even with the addition of [2.2.2] the solubility of $NaCH_3SO_3$ in the polymer does not approach that of $NaCF_3SO_3$ in the absence of [2.2.2]. Whereas the complex $aPEO_8NaCF_3SO_3$ is totally amorphous, the complex $aPEO_8(NaCH_3SO_3$:[2.2.2]) has undissolved salt, that can be seen visually.

The driving force for salt complexation in polymer electrolytes is the strong solvation energy of the cation by the polymer, which overcomes the lattice energy of the salt providing that the lattice energy is not too large.[27] When the cation is complexed by the cryptand the solubility of the cryptand–anion salt is now dependent upon more subtle dielectric and solvation phenomena. (Smid has compared the equilibrium constants of alkali-metal complexation by immobilized crown ethers and immobilized straight-chain polyethers. Although highly solvent dependent, the equilibrium constant for crown-ether complexation is generally 100 times greater than that observed for linear polyethers.[28] Cryptands are known to complex alkali-metal cations even more strongly.[22]) There is no strong interaction between the polymer and the anion in these systems, and in the absence of strong polymer–cation complexation, the salt may be no longer soluble. Precipitation of normally soluble salts has also been observed for nonaqueous solutions of cryptand or crown ether complexed salts.[29] It may be possible to suppress salt crystallization in polymer–salt complexes where the anion can interact more strongly with the polymer, such as the $(CH_2CH_2NH)_xNaCF_3SO_3$ systems studied by Harris, where evidence was found for hydrogen bonding between the polymer and the anion.[30]

The DSC traces of the cryptand–polymer salt complexes are all virtually identical, displaying a glass transition, a cold crystallization, and melting exotherms, that are similar to but broader than those observed for aPEO (Table I). The polymer cannot effectively compete with the complexation ability of the cryptand, and consequently the salt does not strongly influence the thermal properties of the polymer. A melting-point depression that would be expected on the basis of colligative properties is not observed, but the expected shift in melting temperature may be obscured by the observed width of the melting transitions. The behavior of these complexes differs from that observed in the poly(phosphazene sulfonate)–cryptand systems, where the addition of the cryptand [2.2.2] did not change the thermal properties of the polyelectrolytes.[11]

Vibrational Spectroscopic Investigation of Cryptand Complexes. The most interesting changes upon [2.2.2] or 15C5 addition to these polymer–salt complexes occur in the Raman spectra (Figure 4). The electrolytes with [2.2.2] or 15C5 have a new sharp band at approximately 850 cm^{-1} overlapping the broad band from the polymer. Sato has observed this band in crystalline alkali-metal crown ether salts and assigns it as an $M–O_n$ breathing motion of the cation inside the crown ether.[31] Papke also observed a similar band in complexes of PEO with alkali-metal salts.[32] Because the frequency of this

(26) Irish, D. E.; Tang, S. Y.; Talts, H.; Petrucci, S. *J. Phys. Chem.* **1979**, *83*, 3268.

(27) Papke, B. L.; Ratner, M. A.; Shriver, D. F. *J. Electrochem. Soc.* **1982**, *129*, 1694.
(28) Xu, W. Y.; Bruno, R.; Smid, *J. Macromolecules* **1985**, *18*, 2061.
(29) Pedersen, C. J.; Frensdorff, H. K. *Angew. Chem.* **1972**, *11*(1), 16.
(30) Harris, C. S.; Ratner, M. A.; Shriver, D. F. *Macromolecules* **1987**, *20*, 1778.
(31) Sato, H.; Kusumoto, Y. *Chem. Lett.* **1978**, 635.

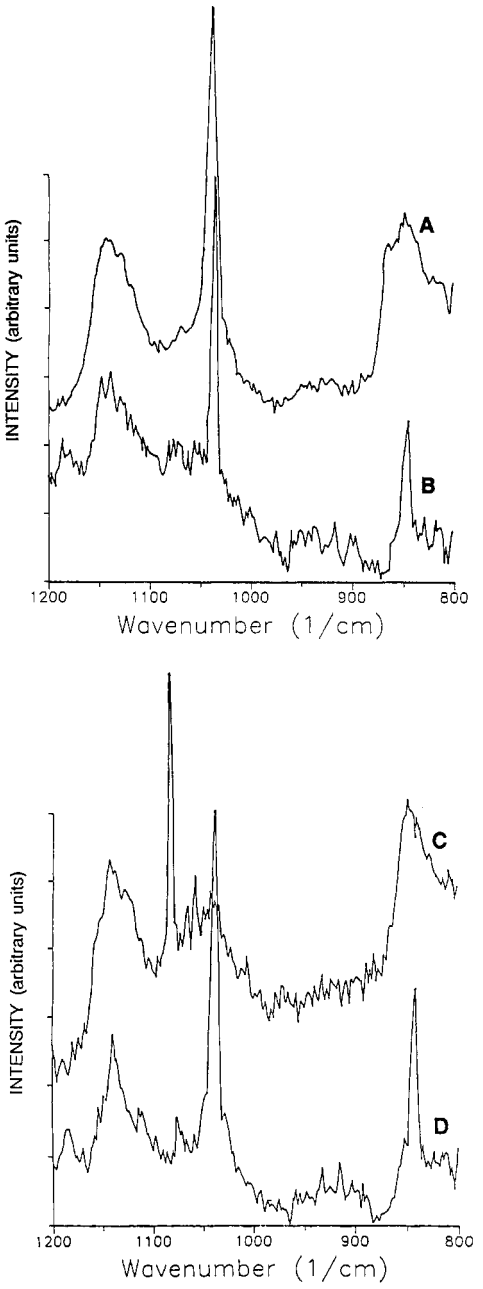

Figure 4. Comparison of Raman spectra of aPEO complexes without [2.2.2] and with [2.2.2] added: (A) $aPEO_{25}NaCF_3SO_3$, (B) $aPEO_{25}(NaCF_3SO_3{:}[2.2.2])$, (C) $aPEO_{25}NaCH_3SO_3$, (D) $aPEO_{25}(NaCH_3SO_3{:}[2.2.2])$.

band is rather high for a simple M–O breathing mode, this vibration may be strongly mixed with CH_2 rocking modes that are also observed in this region. The polymer PEO and many of its complexes are semicrystalline, and the CH_2 rocking modes are quite sharp; the additional band due to the $M–O_n$ breathing mode in these complexes was thus well-resolved. By contrast, the Raman bands of aPEO are quite broad and probably obscure the band due to the $M–O_n$ breathing vibration. The addition of cryptand or crown ether also shifts the SO_3 symmetric stretch in salt complexes (Table II). The shift for the $NaCH_3SO_3$ complex of 40 cm^{-1} upon addition of cryptand is much more dramatic than that of the $NaCF_3SO_3$ complexes (7 cm^{-1}), indicating that the addition of the cryptand greatly changes the local environment about the $CH_3SO_3^-$. The

(32) Papke, B. L.; Ratner, M. A.; Shriver, D. F. *J. Phys. Chem. Solids* **1981**, *42*, 493.

Table II. Position of SO_3 Symmetric Stretch in aPEO Complexes of $NaCF_3SO_3$ and $NaCH_3SO_3$

complex	res, cm^{-1}	complex	res, cm^{-1}
$NaCF_3SO_3$(s)	1067	$aPEO_{25}(NaCF_3SO_3{:}[2.2.2])$	1037
$NaCH_3SO_3$(s)	1085	$aPEO_{25}(NaCF_3SO_3{:}(15C5))$	1037
$aPEO_{25}NaCF_3SO_3$	1043	$aPEO_{25}(NaCH_3SO_3{:}[2.2.2])$	1042
$aPEO_8NaCF_3SO_3$	1043, 1056	$aPEO_{25}(NaCH_3SO_3{:}(15C5))$	1081
$aPEO_{25}NaCH_3SO_3$	1085		

Table III. Conductivity of aPEO and Its Complexes

polymer	σ(40 °C), S cm^{-1}	σ(80 °C), S cm^{-1}
aPEO	1.6×10^{-7}	7.2×10^{-7}
$aPEO_{25}NaCF_3SO_3$	6.7×10^{-5}	3.3×10^{-4}
$aPEO_{12}NaCF_3SO_3$	2.4×10^{-5}	3.2×10^{-4}
$aPEO_8NaCF_3SO_3$	1.4×10^{-5}	1.6×10^{-4}
$aPEO_{25}NaCH_3SO_3$	2.7×10^{-7}	1.3×10^{-6}
$aPEO_{25}NaBF_4$	7.7×10^{-5}	3.7×10^{-4}
$aPEO_{25}NaI$	7.8×10^{-5}	5.9×10^{-4}
$aPEO_{25}NaSCN$	7.1×10^{-5}	4.3×10^{-4}
$aPEO_{25}(NaCF_3SO_3{:}[2.2.2])$	3.0×10^{-6}	1.3×10^{-5}
$aPEO_{25}(NaCF_3SO_3{:}0.5[2.2.2])$	3.0×10^{-5}	1.6×10^{-4}
$aPEO_{25}(NaCF_3SO_3{:}(15C5))$	9.1×10^{-6}	7.8×10^{-5}
$aPEO_{25}(NaCH_3SO_3{:}[2.2.2])$	3.3×10^{-6}	1.6×10^{-5}
$aPEO_{25}(NaCH_3SO_3{:}0.5[2.2.2])$	1.6×10^{-6}	1.2×10^{-5}
$aPEO_{25}(NaCH_3SO_3{:}(15C5))$	2.4×10^{-6}	4.8×10^{-6}
$aPEO_{25}(NaBF_4{:}[2.2.2])$	2.1×10^{-6}	7.7×10^{-6}
$aPEO_{25}(NaI{:}[2.2.2])$	4.1×10^{-7}	1.9×10^{-6}
$aPEO_{25}(NaSCN{:}[2.2.2])$	1.9×10^{-6}	8.8×10^{-6}

shift for the crown ether–$NaCH_3SO_3$ complex is very small (ca. 4 cm^{-1}). These results indicate that the nearly spherical cryptand much more effectively screens the ions from each other than the more open crown ether. This is not surprising as many structural studies of alkali-metal crown ether salts show the anion within bonding distance of the alkali-metal cation.[33] The present results demonstrate that the cation is best segregated from the anion in the following order: polymer < crown ether < cryptand.

The addition of cryptand sharpens infrared spectrum of the NaSCN complex in the CN stretching region (fwhm = 15 cm^{-1}) but does not shift the band.

Ionic Transport Studies. The complex impedance data show significant conductivities for the parent polymer electrolytes (Table III). (Previous studies on other polar polymers indicate that salt impurities are responsible for the observed conductivity of the supposedly pure host polymer.) The conductivity of the $aPEO_{25}NaCH_3SO_3$ is quite low compared to analogous complexes of the other salts. This is most likely due to the limited solubility of $NaCH_3SO_3$ in the polymer as indicated by X-ray diffraction.

A maximum in conductivity with increasing salt concentration is a phenomenon commonly observed in polymer electrolytes.[3,4,7,32] The monotonic decrease in conductivity observed for the $NaCF_3SO_3$ complexes may arise from a conductivity maximum for these systems below the lowest salt concentration 1 salt formula unit/25 EO units. The maximum for the corresponding $LiCF_3SO_3$ series for aPEO occurs at $aPEO_{25}LiCF_3SO_3$.[7]

The observation of a conductivity maximum can be rationalized by considering the VTF model for ion motion and the conductivity equation (eq 1).

$$\sigma = \sum n_i q_i \mu_i = \sum \sigma_i \quad (1)$$

This equation relates the total conductivity σ, to the conductivity of each charge carrier, σ_i, its concentration,

(33) Truter, M. R. *Struct. Bonding* **1973**, *16*, 71.

n_i, its ionic mobility, μ_i, and the absolute value of the charge it carries, q_i. The total concentration of charge carriers, $\sum n_i$, will include all charged species but not ion pairs. Vincent has shown for salt solutions of low molecular weight PEO that the concentration of ion pairs and charged ion aggregates rises more rapidly than the concentration of free ions as salt concentration is increased;[10] thus the fraction of free ions will be reduced at high concentration. The charge of the ions, q, should be unity for all charge carriers. The ionic mobility of a carrier, μ_i, is dependent upon two factors: the polymer segmental motion and the size of the ion. As more salt is added to the polymer, the observed T_g increases (Table I). As T_g increases, the segmental motion at a given temperature is reduced, and since ion diffusion is strongly coupled to polymer segmental motion, the mobility of the smaller free ions falls.[34]

The dependence of μ_i and also σ_i on ion size is reflected in the Stokes–Einstein equation (eq 2) and the Nernst–

$$D_i = \frac{k_B T}{6\pi\eta r_i} \quad (2)$$

$$\sigma_i = \frac{D_i n_i q_i^2}{k_B T} \quad (3)$$

Einstein relationship (eq 3).[35] The diffusion coefficient, D_i, of the charge carrier is inversely proportional to the viscosity of the medium, η, and the radius of the ion, r_i. Thus larger ions have smaller diffusion coefficients and should contribute less to the conductivity. Free ions that are strongly coordinated to the polymer may be less mobile than the larger, but less strongly coordinated, ion aggregates. Increasing the salt concentration should lead to the formation of large low-mobility ion aggregates (as indicated by the Raman data) and also to a reduction in the mobility all ions due to increase in T_g and in viscosity, η[13b,c] This general fall in ionic mobility would explain the observed decrease in the conductivity.

The conductivity of the electrolytes is affected differently by addition of complexing agents. As cryptand is added to the $aPEO_{25}NaCF_3SO_3$ complex the conductivity at 40 °C falls dramatically until a cation–cryptand ratio of 1:1 is reached. Addition of crown ether also results in a decrease in the conductivity, but the decrease is smaller. By contrast, the addition of cryptand to the $NaCH_3SO_3$ complexes enhances the conductivity, although this enhancement is less pronounced than the fall for the $NaCF_3SO_3$ complexes. When the concentration of Na^+ and cryptand are equal, the conductivities of the $NaCH_3SO_3$–cryptand and the $NaCF_3SO_3$–cryptand complexes are virtually identical. The complexes of the other salts show a decrease in conductivity similar to that observed for the $NaCF_3SO_3$ complex upon addition of cryptand. The conductivity of the complex with the smallest ion, I^-, falls the most dramatically (Table III). The addition of crown ether to the $NaCH_3SO_3$ complex also enhances the conductivity, and at 40 °C this enhancement is almost equal to that of the cryptand complex but is not as great at higher temperatures.

Similar behavior occurs upon addition of cation complexing agents to nonaqueous salt solutions. The changes in the conductance of these solutions is dependent upon the system: a slight decrease in conductance can be as-

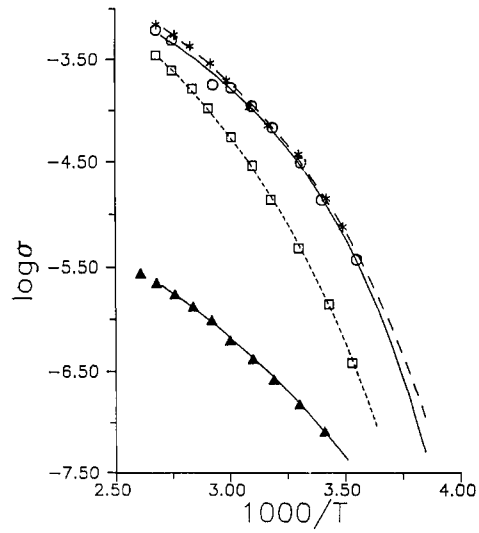

Figure 5. Temperature-dependent conductivity for polymer–salt complexes of aPEO: ○, $aPEO_{25}NaCF_3SO_3$; *, $aPEO_{25}NaSCN$; □, $aPEO_8NaCF_3SO_3$; ▲, $aPEO_{25}NaCH_3SO_3$. Lines are data fitted to the VTF equation.

cribed to a decrease in ionic mobility due to the larger size of the compound cation, whereas large variations in conductance may arise from changes in the solubility of salt in the solvent accompanied by dissolution or precipitation.[29,36]

Precipitation of the cryptand–salt complex probably causes the dramatic decrease in the conductivity for the complexes of $NaCF_3SO_3$, $NaBF_4$, NaI, and NaSCN when cryptand is added. The fall in conductivity is much greater than expected from a simple decrease in the cation mobility due to cryptand complexation. A large proportion of the conductivity in the parent complexes is probably due to anion conduction. The mobility of the free anion would be largely unaffected by cryptand addition or should increase. (The T_g's of the polymers fall when cryptand is added (Table I). In the absence of other factors this fall should increase polymer segmental motion and hence anion mobility. The cryptand–Na^+ complex cation may still interact with anions to form a cryptand-separated ion pair or may precipitate as shown by X-ray data (Figure 3). The planar crown ether does not surround Na^+ (as cryptand does) and therefore shields it less extensively from $CF_3SO_3^-$ and the polymer. If the Na^+–crown ether–cation interacts with aPEO, then the formation of crown-ether-separated ion pairs and also the degree of precipitation of $NaCF_3SO_3$ may be reduced. Therefore the observed conductivity for the $NaCF_3SO_3$–15C5 complex is intermediate between that observed for the $NaCF_3SO_3$ complex and the $NaCF_3SO_3$–cryptand complex.

The Raman and X-ray data indicate that the simple salt $NaCH_3SO_3$ is poorly solvated by the polymer. The addition of the cryptand to this complex increases the solubility of the salt in the polymer. Upon dissolution of the salt both the complex cation and the anion are released for conduction. (Transference number studies for simple PEO complexes indicate that in general, more than half of the charge is carried by the anion.)[37] The Raman data indicate that the crown ether is not as effective at segregating the cation and anion as the cryptand. The con-

(34) Gibbs, J. H.; Adam, G. J. *J. Chem. Phys.* **1965**, *43*, 139.
(35) Smedley, S. I. *The Interpretation of Ionic Conductivity in Liquids*; Plenum Press: New York, 1980.
(36) Kopolow, S.; Mahecek, Z.; Takaki, U.; Smid, J. *J. Macromol. Sci., Chem.* **1973**, *A7*(5), 1015.
(37) (a) Sørensen, P. R.; Jacobsen, T. *Electrochim. Acta* **1982**, *27*, 1671. (b) Bouridah, A.; Dalard, F.; Deroo, D.; Armand, M. B. *Solid State Ionics* **1985**, *18–19*, 287.

Table IV. VTF and Arrhenius Parameters for aPEO Complexes

complex	T_0, K	B, eV	A, S $K^{1/2}$ cm^{-1}	$T_g - T_0$, K	E_a,[c] eV
$aPEO_{25}NaCF_3SO_3$	214	0.053	0.55	10	0.46
$aPEO_{12}NaCF_3SO_3$	211	0.080	3.97	25	0.75
$aPEO_8NaCF_3SO_3$	202	0.092	3.61	42	0.66
$aPEO_{25}NaCH_3SO_3$	178	0.084	0.006	34	0.42
$aPEO_{25}NaBF_4$	207	0.056	0.60	16	0.40
$aPEO_{25}NaI$	207	0.069	2.64	22	0.50
$aPEO_{25}NaSCN$	202	0.068	1.37	25	0.45
$aPEO_{25}(NaCF_3SO_3$:[2.2.2])	154	0.113	0.189	60	0.39
$aPEO_{25}(NaCF_3SO_3$:(15C5))[a]					0.54
$aPEO_{25}(NaCH_3SO_3$:[2.2.2])	154	0.123	0.40	59	0.45
$aPEO_{25}(NaCH_3SO_3$:(15C5))[b]					
$aPEO_{25}(NaBF_4$:[2.2.2])	167	0.084	0.027	31	0.35
$aPEO_{25}(NaI$:[2.2.2])[a]					0.34
$aPEO_{25}(NaSCN$:[2.2.2])	214	0.051	0.011	−6	0.42

[a] Data fit the Arrhenius equation, but not the VTF equation (eq 2). [b] Data fit neither Arrhenius nor VTF equation. [c] Calculated by using the Arrhenius equation (equation 3).

ductivity of the $NaCH_3SO_3$ complex upon addition of (15C5) therefore rises only slightly, as fewer mobile anions are liberated.

The temperature dependence of the ionic conductivity of these polymer–salt complexes is shown in Figure 5. The parent complexes give gently curving Arrhenius plots. This phenomenon is commonly observed in amorphous polymer electrolytes, and the temperature dependence can be fitted by the Vogel–Tammann–Fulcher equation (eq 4). T_0 is

$$\sigma = AT^{-1/2}e^{-B/((k_B(T-T_0))} \quad (4)$$

an empirical parameter related to the glass transition temperature of the polymer (empirically in polymer electrolytes $T_0 \sim T_g - 50$), B is a pseudo-activation energy and is related to the expansivity of the polymer required for ion migration, and the preexponential factor, A, is dependent on the concentration of charge carriers. Alternatively the conductivity data can be fit by the Arrhenius equation (eq 5).

$$\sigma = A'T^{-1}e^{-E_a/(k_BT)} \quad (5)$$

The fitted data in Figure 5 indicate good agreement with the VTF relation; however, the values of T_0 are imprecise because of the limited temperature range available to us. The T_0's obtained for its of these data vary quite widely: in some cases the best fit is obtained for a T_0 that exceeds T_g. In addition, temperature-dependent precipitation of salt from some of these complexes probably contributes strongly to the deviation from the expected temperature dependence for the conductivity.

It thus appears that while the changes in elasticity and T_g upon addition of crown or cryptand can affect conductivity, the dominant behavior can be described simply in terms of effective carrier number. The dominant charge carriers are assumed to be anions (t_- ca. 0.6 or more). In a complex such as $NaCF_3SO_3$.PEO, the cation–anion interaction is weak, and the number of free anions is likely to be relatively large. Addition of cryptand or crown ether breaks up the cation solvation by the polyether, and it also more effectively separates cations and anions. In the case of the NaSCN, $NaBF_4$, and $NaCF_3SO_3$, this results in phase separation, fewer free anions, and a low conductivity prefactor. In the case of $NaCH_3SO_3$, addition of crypt or crown breaks up the ion pairs but does not bring about precipitation so the conductivity is enhanced. These trends are reflected in the prefactors A or eq 4 and Table IV; A is proportional to carrier number, and with the strongly ion-pairing $CH_3SO_3^-$ anion, A increases with cryptand addition, while for the more weakly ion paired (better solvated) SCN^-, $CF_3SO_3^-$, or BF_4^- anions, the A constant drops as cryptand is added.

Acknowledgment. K.E.D. thanks the NSF for a Predoctoral Fellowship. This research was supported by NSF Grant DMR-8821571 through the Northwestern University Materials Research Center and by the U.S. DOE DE-FG02-85ER45220.

Registry No. 15-Crown-5, 33100-27-5; cryptand[2.2.2], 23978-09-8.